First-principles molecular dynamics studies of liquid tellurium

R Stadler and M J Gillan

Physics and Astronomy Department, University College London, Gower Street,
London WC1 6BT, UK

Abstract. First-principles molecular dynamics simulations of liquid tellurium at 1123 K and at continuously varied densities are presented. The question of why recent studies within density functional theory overestimated the number of nearest neighbours is analysed in terms of structure factors and contributions of different neighbour shells to the pair distribution functions where the local density approximation and the generalized gradient approximation were used for the exchange–correlation functional. A recently proposed liquid–liquid phase transition under high pressure is also addressed.

1. Introduction

The atomic structure of liquid tellurium (ℓ-Te) has been a much debated topic both from theoretical [1,2] and experimental [3,4] points of view. Unlike liquid selenium, which remains semiconducting up to rather high temperatures where the twofold-coordinated chain structure of the solid is preserved, Te becomes a poor metal upon melting and changes its structure to entangled broken chains [4] with a coordination number of about 2.5 at the melting point ($T_m = 623$ K) and 3 at higher temperatures.

On the basis of neutron scattering experiments, Menelle *et al* [5] suggested a model for the liquid where the first 2.5–3 neighbours are not equivalent and only two of them are covalently bonded whereas the third is only weakly bound to the chain at a slightly larger distance. Although this structure could be reproduced by semi-empirical methods [4,6], density functional theory (DFT) calculations overestimated the coordination number by far: a value of ~6 was found [7,8]. A very surprising aspect of this disagreement with experiment is that it was found for both of the most common approximations for the exchange–correlation functional, namely, the local density approximation (LDA) and the generalized gradient approximation (GGA). Usually, the GGA corrects the results from the LDA, as was found for the structure of liquid selenium [9], or even overcorrects them, as in the case of the equilibrium volume of trigonal Te where the experimental volume was almost exactly in the middle between an underestimated LDA value and an overestimated GGA value [10,11].

Quite recently, a first-order liquid–liquid phase transition at high pressures has been proposed for ℓ-Te as a result of thermal and electrical measurements [12] and density measurements by means of x-ray absorption [13]. Although no drastic change of the structure factor across the proposed phase boundary could be detected [14], an increase of the coordination number was found.

The aim of the present work is to investigate the reason for the disagreement between DFT calculations and experiment, and whether it is related to the existence of two phases in ℓ-Te.

All calculations presented were performed at $T = 1123$ K. This relatively high temperature has been used because the problem that we study is temperature independent and at higher temperatures the systems studied can be equilibrated more efficiently. The particular value of 1123 K has been used because it is the upper bound of the p–T phase diagram in reference [14].

2. Simulation methods

We performed our first-principles molecular dynamics (FPMD) simulations within a DFT framework using the pseudopotential approximation and plane-wave basis sets. All of our calculations were carried out by employing the well-established first-principles simulation code VASP [15–17]. For the construction of the ultrasoft pseudopotential [18] for Te, two energy channels were used for the s and p wavefunctions, and the cut-off radii for the wavefunctions and the augmentation charges were set to 2.90 and 2.59 au, respectively.

An important feature of the present work is that we have employed both the local density approximation (LDA) and the generalized gradient approximation (GGA). The parametrization of Perdew and Zunger [19] has been used for the LDA calculations and the PW91 functional of Perdew and Wang [20] for the GGA calculations.

Our periodically repeated box contained 64 atoms. Using the Nosé–Hoover thermostat technique, the equations of motion were solved with a time step of 3 fs in all systems studied. A total simulation time of 7.5 ps was separated into 2.5 ps for equilibration and 5 ps for the sampling of structure factors and pair distribution functions. In our (N, V, E) calculations the pressure and temperature were allowed to fluctuate, where the time average of the temperature was fixed by our thermostat technique. For the calculation of the pressure, averages have been sampled from MD runs with a total simulation time of 1 ps.

3. Results and discussion

In figure 1 the static structure factor $S(k)$ and the radial distribution function $g(r)$ of ℓ-Te at $T = 1123$ K are compared with neutron diffraction data from reference [5]. For the density ρ, the experimental value of 5.57 g cm^{-3} [21] was chosen.

The static structure factor provides the most direct means of comparison with diffraction data and is derived from

$$S(k) = \langle |\hat{\rho}_k|^2 \rangle \tag{1}$$

in our calculations. Here, the dynamical variable $\hat{\rho}_k$ represents the density of atoms at wave-vector k:

$$\hat{\rho}_k = N^{-1/2} \sum_{i=1}^{N} \exp(i k \cdot R_i) \tag{2}$$

where the sum goes over all N atoms in the system.

From figure 1 it can be seen that the choice of the exchange–correlation functional does not influence the results a lot for this particular combination of temperature and density. The results from GGA and LDA give almost identical curves for $S(k)$ and only small differences for its Fourier transform, the radial distribution function $g(r)$. The first maxima of $g(r)$ from GGA and LDA are identical in position and width; the first minimum is deeper and more pronounced within LDA. If the results are now compared with the neutron diffraction data from reference [5] shown as dotted lines in figure 1, for $S(k)$ the measured and calculated data fit together quite well, although there are discernible shifts especially in the wavelength area from 3 to 6 Å^{-1}. Unfortunately, this is the region where covalent bonding occurs and,
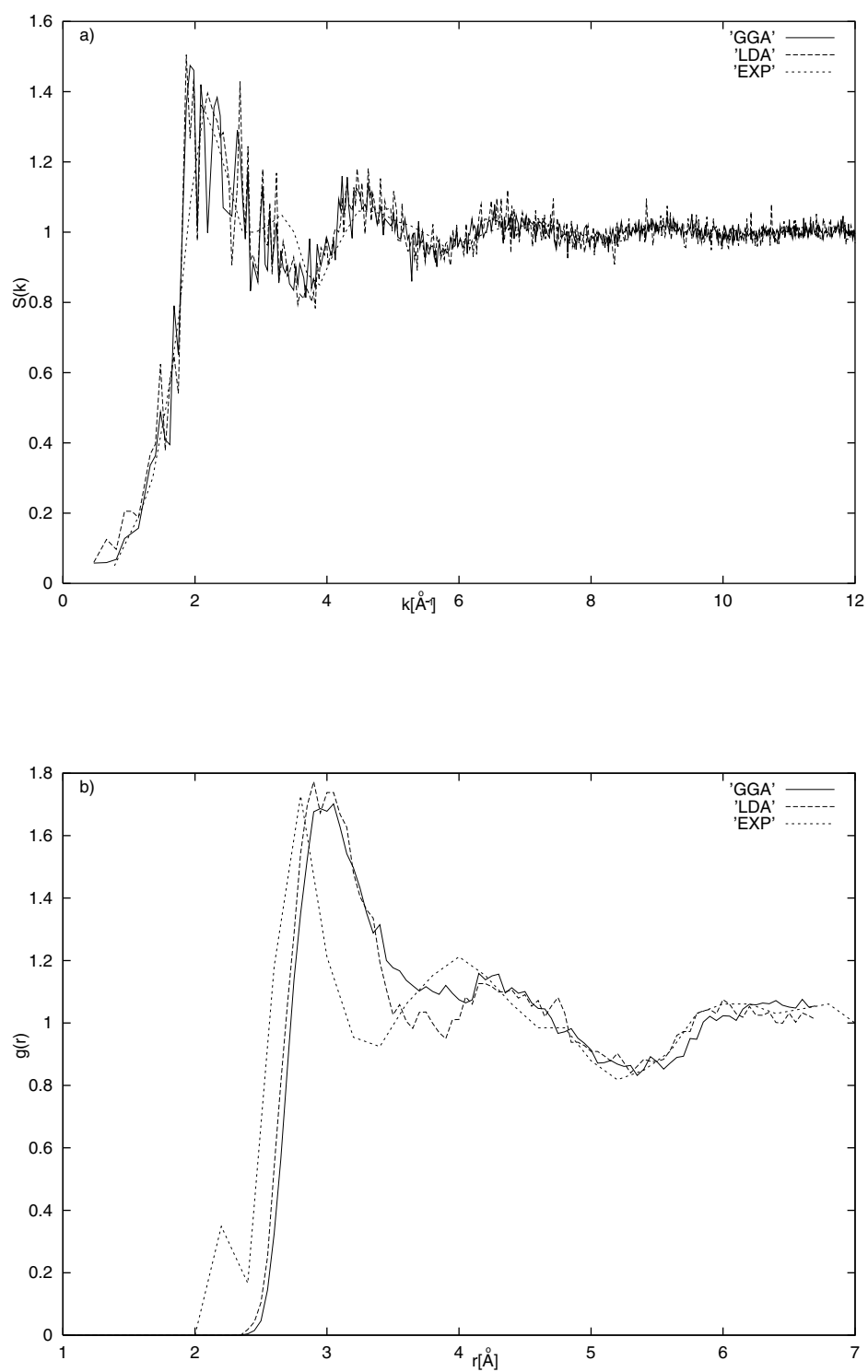
Figure 1. (a) The structure factor $S(k)$ and (b) the radial distribution function $g(r)$ for ℓ-Te at $T = 1123$ K and $\rho = 5.57$ g cm^{-3}, GGA results are given as solid lines, LDA results as dashed lines and neutron scattering data (reference [5]) as dotted lines.

consequently, the radial distribution function derived from diffraction experiments looks very different from our calculated ones (figure 1(b)). The first maximum and minimum of $g(r)$ occur at lower distances in the neutron diffraction data and also the width of the first peak is smaller. The disagreement is further illustrated in table 1 where average coordination numbers N_c are listed and the first line corresponds to the experimental density. In all cases the cut-offs r_c have been chosen to be identical with the first minima of $g(r)$ and are given in parentheses in table 1, and it can be found that N_c is largely overestimated by both sets of our calculations.

Table 1. Coordination numbers N_c calculated from GGA and LDA and from neutron diffraction [5] for two different densities. The cut-off radii r_c which were chosen to be the first minima of $g(r)$ are given in parentheses.

ρ (g cm^{-3})	GGA	LDA	Experiment
5.57	4.81 (3.70)	4.00 (3.50)	2.67 (3.35)
4.46	2.85 (3.40)	3.98 (3.60)	—

It is not surprising that LDA calculations give too high a value of N_c, since also for solid tellurium in its trigonal structure the interchain interactions are overestimated and the equilibrium volume therefore is found at a lower value than in experiment as studied and analysed in detail in references [10] and [11]. This same overestimation of interchain bonding results now in a far too high number of neighbours in the liquid. For the GGA calculations the
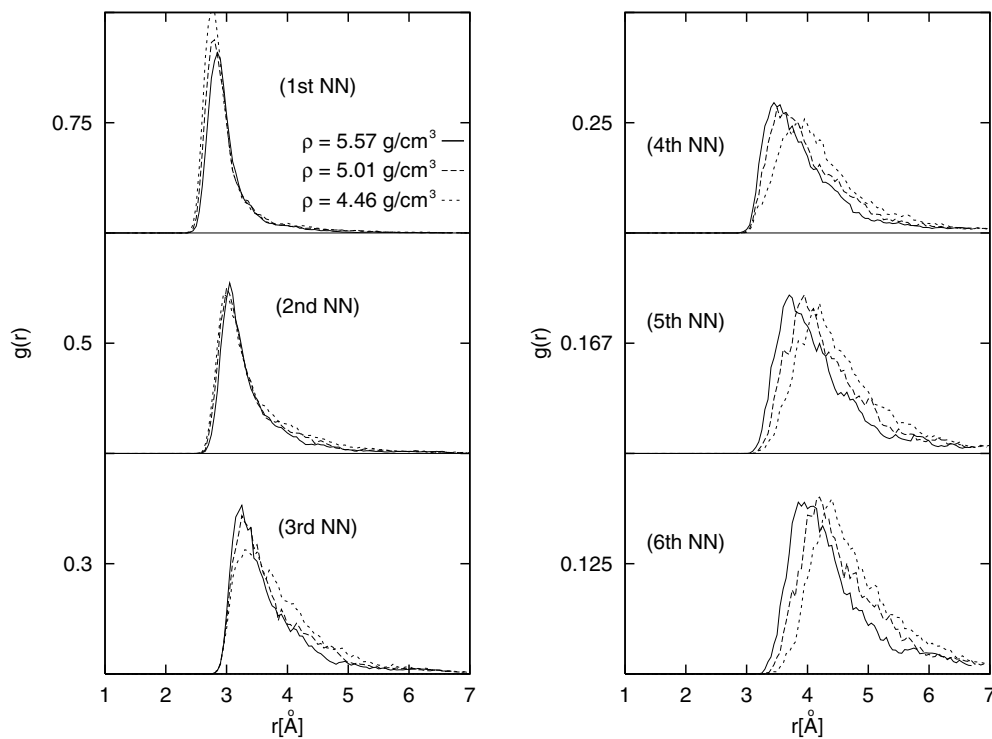

Figure 2. Individual contributions to the radial distribution function $g(r)$ for ℓ-Te at 1123 K calculated using the GGA; $\rho = 5.57$ g cm^{-3} (solid lines), 5.01 g cm^{-3} (dashed lines), 4.46 g cm^{-3} (dotted lines).

case is less obvious, since the interchain bonding of trigonal Te (t-Te) is underestimated within this approximation [11]. Quite unusually compared with other systems, gradient corrections are considerably overcorrecting the deficiencies of the LDA reference for t-Te and GGA calculations give a value for its equilibrium volume that is as much too high as the LDA value is too low. Therefore it seems surprising that GGA should overestimate the number of neighbours within the liquid. If on the other hand as claimed in references [12–14] there are a low-pressure and a high-pressure phase in the liquid, MD calculations performed at the experimental density within the GGA might actually describe the system under pressure, since an overestimation of the volume of the solid is likely to result in an underestimation of the equilibrium density in the liquid.

In figure 2 the contributions of the first six neighbours to $g(r)$—calculated by sorting the sequence of neighbours and averaging their distance from the central atom over all configurations and all atoms—are depicted separately for GGA calculations at the experimental density (solid lines) and a density reduced by 10% (dashed lines) and 20% (dotted lines). It is interesting to see that for the first two neighbours, the ones covalently bonded inside the chains, there is not much change in the position and shape of the main peak if different densities are compared other than the peak height of the first neighbour peak slightly rising. In the case of the third neighbour which is usually believed to be the link in a branched network [4], the peak broadens distinctly when density decreases. The three following neighbour atoms show a completely different behaviour. All of them are moving away from the central atom with
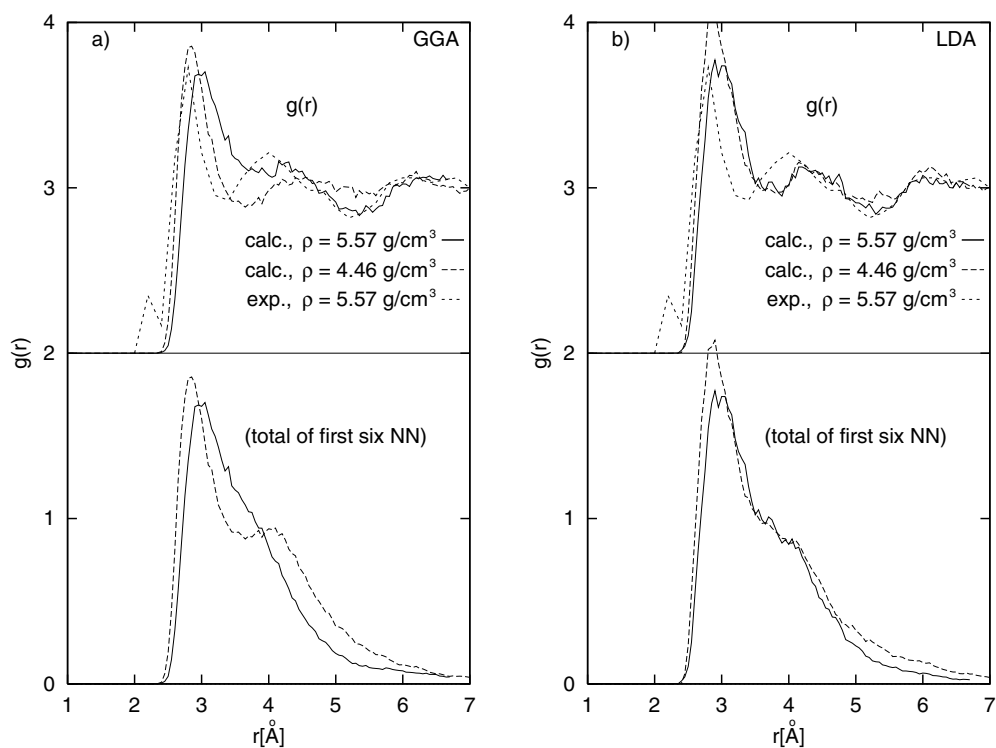

Figure 3. The radial distribution function $g(r)$ for ℓ-Te at 1123 K (upper panels) and the sum over contributions of the first six neighbours (lower panels), calculated using (a) GGA and (b) LDA, for densities $\rho = 5.57$ g cm^{-3} (solid lines) and 4.46 g cm^{-3} (dashed lines). Neutron scattering data [5] for $\rho = 5.57$ g cm^{-3} are also shown (dotted lines).

decreasing density indicating that their bonding is indeed pressure induced.

Figure 3(a) compares $g(r)$ and the summed contribution of the first six nearest neighbours calculated for the experimental density and a density reduced by 20% within the GGA. For the reduced density, $g(r)$ is resembling the experimental curve distinctly more in position, height and width of the first peak. The summed contributions show that the third-, fourth- and sixth-nearest neighbours have moved to the second maximum of $g(r)$ which they did not do at the experimental density. Also LDA calculations have been performed at the lowered density just to prove the point that a density decrease is not a remedy in this case, because our considerations are based on the volume overestimation for the solid, which LDA is underestimating. The radial distribution functions in figure 3(b) show that within LDA indeed only the size of the first maximum of $g(r)$ is increasing, which is a consequence of the fact that $g(r)$ is scaling with the volume per atom in any system. The peak positions and shapes are unaffected by the change in density within the LDA.

These differences in the density dependences of GGA and LDA results can also be seen from the second line of table 1 which lists N_c for the reduced density. Whereas the GGA value comes very close to the experimental one, the value calculated within the LDA differs only slightly from that at the experimental density.

Figure 4 shows the static structure factors $S(k)$ from GGA and LDA at the reduced density, where both curves show an improved agreement with the experimental one in the wavelength area between 4 and 6 Å^{-1} compared with figure 1(a), although the disagreement below $k = 4$ Å^{-1} remains. Not surprisingly, within LDA $S(k)$ exhibits high values at low wavevectors for the reduced density. This indicates a highly compressible liquid since the
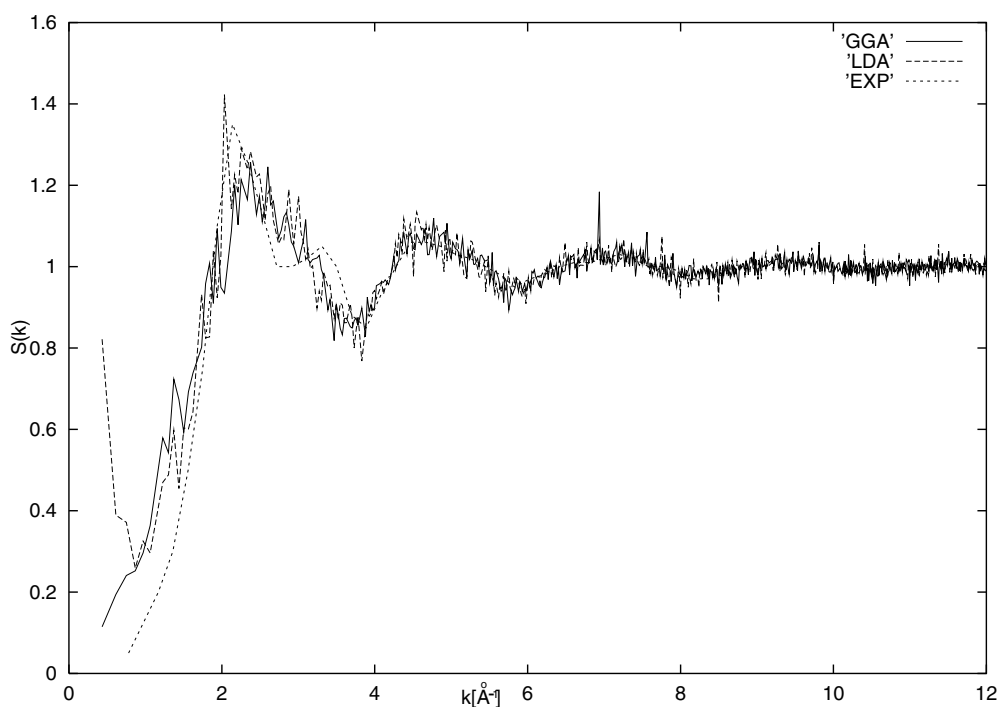

Figure 4. The structure factor $S(k)$ for ℓ-Te at $T = 1123$ K and $\rho = 4.46$ g cm^{-3}; GGA results are given as solid lines, LDA results as dashed lines. Neutron scattering data [5] for $\rho = 5.57$ g cm^{-3} are also shown (dotted lines).
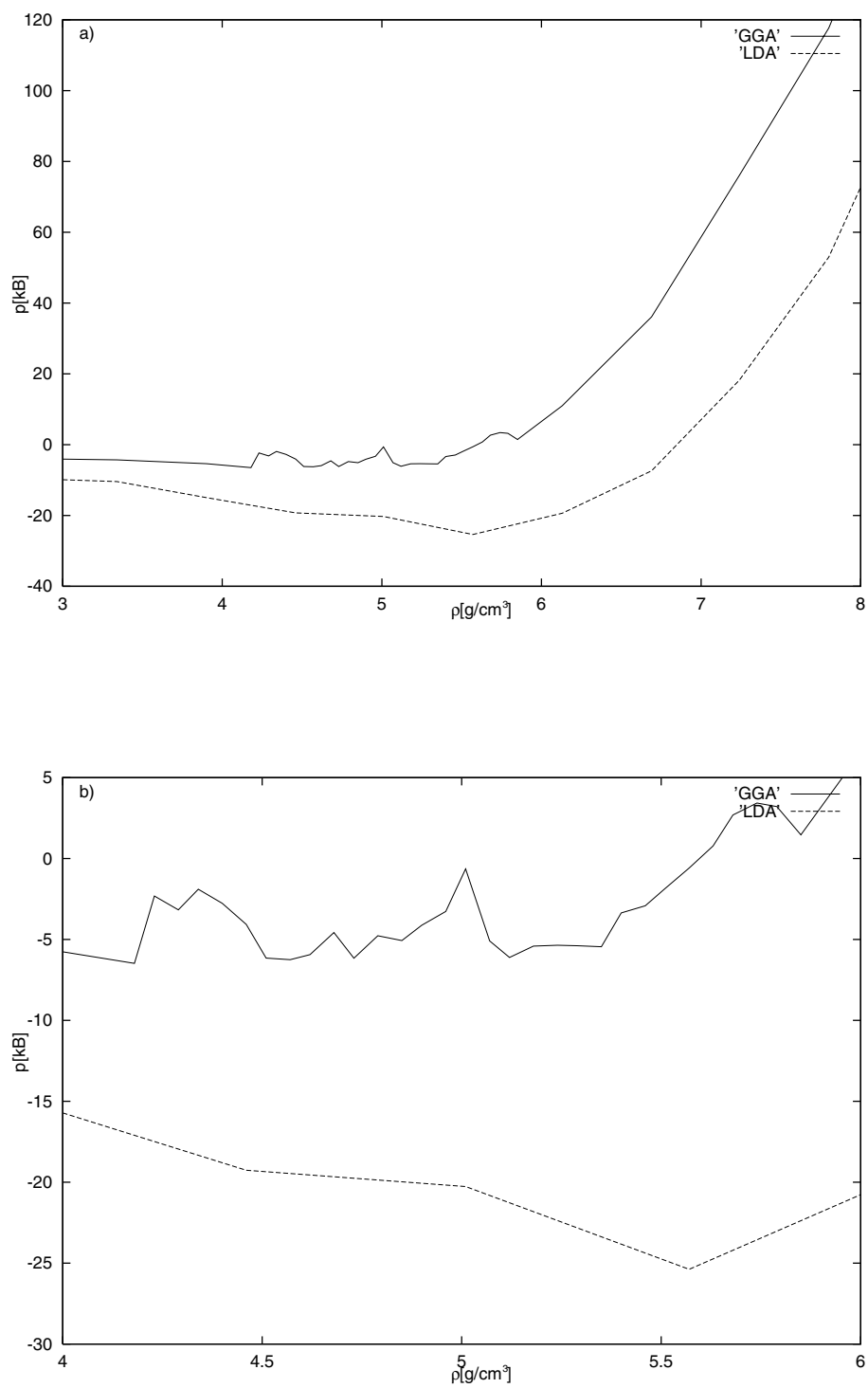
Figure 5. Pressure for (a) larger and (b) smaller ranges of densities around the experimental equilibrium value of 5.57 g cm^{-3} calculated using GGA (solid lines) and LDA (dashed lines).

isothermal compressibility κ_T is related to the static structure factor by

$$\lim_{k \to 0} S(k) = nk_B T\kappa_T \qquad (3)$$

where n is the number density and k_B is Boltzmann's constant. This can be understood as a consequence of LDA overbinding, because the experimental density must be considered as reduced already compared to the LDA equilibrium, since the volume of t-Te was underestimated within this approximation. Therefore, if the density is further reduced, the high compressibility of the liquid becomes reflected in $S(k)$. For LDA calculations of ℓ-Se, the same behaviour was encountered at its experimental density [9].

If we are correct that within GGA at the experimental density the high-pressure phase proposed in references [12–14] is found and that one has to go to lower densities to find the low-pressure phase, this must be reflected in the dependence of the pressure on the density. Figure 5 shows this dependence calculated from GGA and LDA for a large scale of densities. Within LDA, zero pressure and therefore an equilibrium state is only reached at a density which is about 25% higher than the experimental one. It is not to be expected that N_c would be reduced to lower values at that density, when atoms are pressed more closely together compared to the case for the experimental density. The GGA curve on the other hand shows local maxima (solid line in figure 5(b)) where the pressure comes close to zero, indicating the possibility of stable phases at different densities. However, since our description of the pressure dependence on the density is influenced by statistical noise, details of figure 5(b) should not be overinterpreted.

4. Conclusions

In summary, we performed FPMD calculations for ℓ-Te at 1123 K at various densities. The ability of DFT within the framework of GGA and LDA to describe this system was critically analysed. As in the somewhat similar case of ℓ-Se [9], LDA was found to give very poor results also for ℓ-Te. Within the GGA, however, the density has to be reduced compared to the experimental one, in order to achieve correct results. This is due to the overestimation of the equilibrium volume of t-Te and is likely to be related to the existence of low-pressure and high-pressure phases of the liquid, which was recently suggested from thermal and electrical measurements [12] and density measurements by means of x-ray absorption [13].

Acknowledgments

References

[1] Enderby J E and Barnes A C 1990 *Rep. Prog. Phys.* **53** 85
[2] Endo H 1993 *J. Non–Cryst. Solids* **156–158** 667
[3] Cabane B and Friedel J 1970 *J. Physique* **32** 73
[4] Hafner J 1990 *J. Phys.: Condens. Matter* **2** 1271
[5] Menelle A, Bellisent R and Flank A M 1987 *Europhys. Lett.* **4** 705
    Menelle A, Bellisent R and Flank A M 1989 *Physica* B **156+157** 174

[6]   Bichara C, Raty J Y and Gaspard J P 1996 *Phys. Rev.* B **53** 206
      Bichara C, Raty J Y and Gaspard J P 1996 *J. Non-Cryst. Solids* **205–207** 361
[7]   Kirchhoff F 1993 *Diploma Thesis* Ecole Polytechnique Fédérale de Lausanne
[8]   Kresse G 1999 Private communications
[9]   Kirchhoff F, Kresse G and Gillan M J 1998 *Phys. Rev.* B **57** 10 482
[10] Kirchhoff F, Binggeli N, Galli G and Massidda S 1994 *Phys. Rev.* B **50** 9063
[11] Kresse G, Furthmüller J and Hafner J 1994 *Phys. Rev.* B **50** 13 181
[12] Brazhkin V V, Voloshin R N, Popova S V and Umnov A G 1992 *J. Phys.: Condens. Matter* **4** 1419
[13] Katayama Y, Tsuji K, Kanda H, Nosaka H, Yaoita K, Kikegawa T and Shimomura O 1996 *J. Non-Cryst. Solids* **205–207** 451
[14] Kenichi Y, Tsuji K, Katayama Y, Koyama N, Kikegawa T and Shimomura O 1993 *J. Non-Cryst. Solids* **156–158** 157
[15] Kresse G 1995 *J. Non-Cryst. Solids* **193** 222
[16] Kresse G and Furthmüller J 1996 *Phys. Rev.* B **54** 11 169
[17] Kresse G and Furthmüller J 1996 *Comput. Mater. Sci.* **6** 15
[18] Vanderbilt D 1990 *Phys. Rev.* B **41** 7892
[19] Perdew J P and Zunger A 1981 *Phys. Rev.* B **23** 5048
[20] Wang Y and Perdew J P 1991 *Phys. Rev.* B **44** 13 298
[21] Thurn H and Ruska J 1976 *J. Non-Cryst. Solids* **22** 331